This article has been accepted for publication in a future issue of this journal, but has not been fully edited. Content may change prior to final publication. Citation information: DOI 10.1109/LCSYS.2020.3044261, IEEE Control Systems Letters

Controller Design for Time-varying Sampling, Co-Regulated Systems

Xinkai Zhang and Justin Bradley

***Abstract*— "Co-regulation" is a time-varying periodic sampling strategy wherein the sampling rate is dynamically adjusted in response to the performance of the controlled system. The controller for co-regulated system needs to adjust control outputs corresponding to the current (changing) sampling rate. This makes performance guarantees such as stability difficult to obtain. In this paper we develop two stability guaranteed control algorithms for co-regulated systems. First is a correct-by-construction stabilizing controller where the control gain matrices are pre-computed offline for a set of sampling rates. This method allows for arbitrary switching of the sampling rates but as a result can be overly conservative. Then a hybrid Model Predictive Control (MPC) algorithm is tailored for co-regulated systems where both the system state trajectory and the sampling rate (scheduling parameter) trajectory are predicted within the receding horizon. The performances of the proposed controllers are demonstrated and discussed for a co-regulated multicopter Unmanned Aircraft System (UAS). The results show co-regulation can efficiently reallocate computational resources based on control performance by varying the sampling rate at runtime, while the proposed control strategies can guarantee co-regulated system stability when working under a time-varying sampling rate.**

***Index Terms*— Sampled-data control, Time-varying systems, Lyapunov methods, Control applications**

I. Introduction

THE computational challenges presented by the new generation of autonomous systems requires careful allocation of computational resources to accomplish mission objectives. For control systems this dynamic resource allocation challenge can be met through aperiodic sampling strategies, exemplified by event-triggered control [1], or self-triggered control [2]. We have developed a strategy, "co-regulation," [3] wherein sampling rate and control inputs are simultaneously changed to adjust overall system performance and reallocate computational resources. In co-regulation, a specially designed controller adjusts performance as a function of the sampling rate governed by a "computational controller" that reallocates computation in the form of sampling rate to the controller based on performance.

The novelty of co-regulation is in its coupling of computational and physical systems via equations of motion rather than incorporating the delays of motion into the models used for task scheduling. In this way, the controller is designed to depend on the changing sampling rate, and the sampling rate is designed to depend on system performance. Different from conventional self-triggered control wherein the sampling interval is decided by complex, online optimization [4], co-regulation calculates the sampling rate trajectory via a separate computational feedback controller that can be executed extremely fast (i.e., $O(1)$ complexity) with negligible resource consumption much like a PID controller [3]. Co-regulation serves as the basis for developing the required mathematical, real-time scheduling, and time-varying controller foundations needed to build a more complete resource-aware, cyber-physical autonomy.

Designing controllers for co-regulated systems presents new challenges because traditional computer-based controllers correspond to a single sampling rate. Varying that sampling rate results in unpredictable performance. As a result, co-regulated controllers need to adjust their gain to correspond with the time-varying sampling rate. Simultaneously, the computational controller changing sampling rate must respond to the performance needs of the system while avoiding potentially destabilizing sampling rates and still meeting other scheduling deadlines. In previous work [5], a Gain-Scheduled Discrete Linear Quadratic Regulator (GSDLQR) control algorithm was designed for a co-regulated Unmanned Aircraft System (UAS). The stability of the system was analyzed in [6], however, the co-regulated system stability cannot be guaranteed during the control design process. Rather, we can only verify if the designed GSDLQR controller can stabilize a specific system model. In this work, we focus on designing stability-guaranteed controllers based on a general, linear system model. We first provide an explicit approach where an infinite horizon optimal control problem is built for co-regulated systems with customized stability

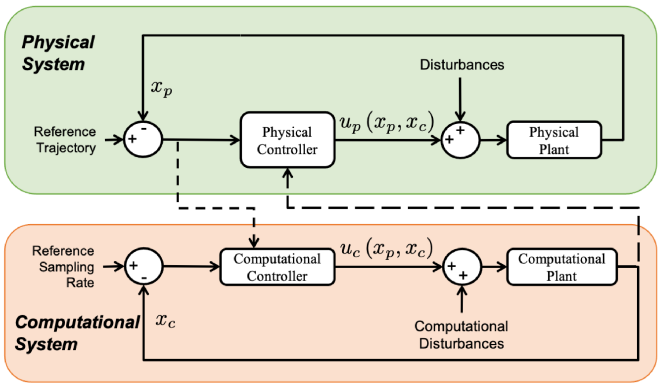

Fig. 1: Co-Regulation Block Diagram [5]

X. Zhang is a PhD Candidate in the Department of Electrical and Computer Engineering, University of Nebraska-Lincoln, USA. xinkai.zhang@huskers.unl.edu

J. Bradley is an Assistant Professor in the Department of Computer Science and Engineering, University of Nebraska-Lincoln, USA. jbradley@cse.unl.edu

constraints. The solution will be a set of gain matrices mapped to each possible sampling rate value and system stability is guaranteed under arbitrary sampling rate switching trajectories. Then we develop a novel co-regulated MPC strategy wherein both the system state trajectory and the sampling rate trajectory are predicted within the receding horizon. This results in a more aggressive control solution for co-regulated systems to handle highly dynamic environments. The effectiveness of the proposed controllers are demonstrated based on a linearized multicopter UAS model [5]. The proposed control strategies can be easily applied to co-regulation design in different application scenarios. The controllers presented here are correct by construction, thereby guaranteeing the safety and stability of the co-regulated system at design time compared with previous control strategies.

II. Co-regulated System Model

Figure 1 shows a block diagram of co-regulation representing an augmented, stacked state-space system

$$\begin{aligned} \dot{x}_p &= Ax_p + Bu_p(x_p, x_c) \\ \dot{x}_c &= u_c(x_p, x_c) \end{aligned} \tag{1}$$

where x_p and u_p are the traditional physical system states and control inputs, x_c is the state representing the sampling rate, and u_c is the computational control input that regulates the sampling rate. In this work we assume the physical system is controllable, and direct feedback of the full states x_p and x_c are available. Output from a computational model representing sampling rate is fed to the physical controller which adjusts physical system performance accordingly. Simultaneously, output from the physical plant is fed to the cyber controller which adjusts sampling rate in response to physical performance [5]. u_p and u_c are functions of both x_p and x_c, thus control performance and sampling rate are directly linked. Since the sampling rate dynamically changes at discrete intervals, the corresponding discrete-time system matrices Φ and Γ become functions of the sampling rate value at each time index, $x_c[k]$. In this work, we focus on the analysis in discrete time because the proposed control algorithms will be implemented in digital computers. The resulting discrete-time-varying system model with respect to time index k is then,

$$x_p[k+1] = \Phi(x_c[k])x_p[k] + \Gamma(x_c[k])u_p[k] \tag{2}$$

and the control input is

$$u_p[k] = u_p(x_p[k], x_c[k]). \tag{3}$$

We can now design a feedback computational control law to calculate the coupled control input u_c, which adjusts the sampling rate, in real time, as the dynamics of the system change. In previous work [5] we presented a computational system control law as

$$u_c[k] = \overbrace{K_{cp}\left\|x_p[k] - x_{p,ref}[k]\right\|}^{\text{pushes rate higher with state error}} - \overbrace{K_c\left(x_c[k] - x_{c,ref}[k]\right)}^{\text{pushes rate towards its reference}}. \tag{4}$$

The coupling gain, K_{cp}, is used to increase the sampling rate of the system in response to physical state error. The gain, K_c, drives x_c toward a desired reference sampling rate $x_{c,ref}$, chosen to minimize resource usage and maintain system stability. $x_{p,ref}[k]$ denotes the physical states reference at time index k. In this work we assume $x_{p,ref} = 0$ to simplify the notation. K_{cp} and K_c are found by employing an optimization scheme that minimizes a cost function composed of custom metrics measuring resource usage, control performance, and energy consumption [5]. Hence at sampling instance k, the discrete-time computational system model can be denoted as

$$\begin{aligned} x_c'[k+1] &= x_c[k] + \frac{1}{x_c[k]}u_c[k] \\ x_c[k+1] &= x_c'[k+1] \text{ rounded to nearest value in } \Sigma, \end{aligned} \tag{5}$$

where $\Sigma = \{f_1, f_2, \ldots, f_N\}$ is a pre-defined finite set that contains stable sampling rate values as prescribed operating points. This limits the sampling rate of the co-regulated system to a finite number to simplify the analysis. The bounds and the resolution of the values in Σ can be customized depending on the application. The general rule to generate Σ is to:

1) set the upper bound based on the system computational bandwidth given all other computing tasks,
2) set the lower bound to the rate where system performance degrades beyond acceptable limits, or otherwise is unstable,
3) set the resolution based on the system dynamics and application scenarios, that can guarantee system stability and accommodate performance requirements, such as disturbance rejection, dynamic response, etc.

The next sampling rate can then be calculated by (4) and (5) based on the current plant states.

III. Explicit Solution - Infinite Horizon Design

We now introduce an Infinite Horizon Control (IHC) design strategy for co-regulated systems that stabilizes the system under arbitrary sampling rate switching trajectories among all possible values in Σ. This will result in a set of explicit gain matrices that can be stored as a look-up table, enabling fast, online implementations. The physical system controller (3) is then $u_p[k] = -K_p(x_c[k])x_p[k]$. The advantage of this IHC design strategy is that the controller synthesis problem can be solved offline without any dependency on the state or sampling rate trajectory.

The physical system model (2) can then be represented as

$$\begin{aligned} x_p[k+1] &= \mathcal{A}(x_c[k])x_p[k], \\ \mathcal{A}(x_c[k]) &= \Phi(x_c[k]) - \Gamma(x_c[k])K_p(x_c[k]). \end{aligned} \tag{6}$$

Then the co-regulated system can be analyzed as a switched system where the sampling rate, x_c, is treated as an arbitrary switching sequence that takes values in the set Σ. Therefore, system evolution will be characterized by an infinite product of closed-loop matrices taken from $\mathcal{A}(x_c)$. The proposed controller in this section will provide control gain matrices $K_p(x_c)$ for each sampling rate in Σ.

A general linear quadratic optimal controller is designed by minimizing the cost function $J = \int_0^\infty (x_p(t)^T Q x_p(t) + u_p(t)^T R u_p(t))dt$, where $Q = Q^T > 0$ and $R = R^T > 0$. Since the sampling rate of the co-regulated system is time-varying, we denote the cost by integrating over the sampling interval trajectory as $J = \sum_{k=0}^{\infty} J[k]$, where

This article has been accepted for publication in a future issue of this journal, but has not been fully edited. Content may change prior to final publication. Citation information: DOI 10.1109/LCSYS.2020.3044261, IEEE Control Systems Letters

$J[k] = \int_{t[k]}^{t[k]+\frac{1}{x_c[k]}} \left(x_p(t)^T Q x_p(t) + u_p(t)^T R u_p(t)\right) dt$. Since the control input $u_p(t)$ is constant over each sampling period, the cost can be equivalently denoted in discrete time as [7]

$$\begin{aligned} J[k] = {} & x_p[k]^T Q_1[k] x_p[k] + 2x_p[k]^T Q_{12}[k] u_p[k] \\ & + u_p[k]^T Q_2[k] u_p[k], \end{aligned} \tag{7}$$

where

$$\begin{aligned} Q_1[k] &= \int_0^{1/x_c[k]} \Phi(\tau)^T Q \Phi(\tau) d\tau, \\ Q_{12}[k] &= \int_0^{1/x_c[k]} \Phi(\tau)^T Q \Gamma(\tau) d\tau, \\ Q_2[k] &= \int_0^{1/x_c[k]} (\Gamma(\tau)^T Q \Gamma(\tau) + R) d\tau, \\ \Phi(\tau) &= e^{A\tau}, \quad \Gamma(\tau) = \int_0^{\tau} e^{A\eta} B d\eta, \end{aligned} \tag{8}$$

A and B are the system matrices in (1). We then seek to calculate the control gain matrices $K_p(x_c), \forall x_c \in \Sigma$ by minimizing the infinite horizon cost function J.

The co-regulated system stability is analyzed by drawing from results in the control community on aperiodic sampling [4] and switched system [8] analysis. In this section we design a correct-by-construction controller to guarantee the asymptotic stability of co-regulated system over all possible sampling rate switching trajectories. The idea of this controller design is based on two arguments:

- The co-regulated system is asymptotically stable if there exists a positive definite Lyapunov function $V(x_p[k], x_c[k]) = x_p[k]^T P(x_c[k]) x_p[k]$ such that $\alpha_1(\|x_p[k]\|) \leq V(x_p[k], x_c[k]) \leq \alpha_2(\|x_p[k]\|)$, and whose difference along the solution of (6) is negative definite. That is, $\Delta V(x_p[k], x_c[k]) = V(x_p[k+1], x_c[k+1]) - V(x_p[k], x_c[k]) \leq -\alpha_3(\|x_p[k]\|)$ can be satisfied $\forall x_p[k] \in \mathbb{R}^n$ and $\forall x_c[k] \in \Sigma$, where $\alpha_1(\cdot)$, $\alpha_2(\cdot)$ and $\alpha_3(\cdot)$ are k_∞ functions [9].
- Since the sampling rate is evolving at runtime and its trajectory is not known in advance, the best we can do is to minimize the upper bound of all possible trajectories. Based on the discrete cost function at each sampling interval (7), we denote the upper bound cost value as $J_{coreg} = \sum_{k=0}^{\infty} \max_{x_c[k] \in \Sigma} J[k]$. Thus, J_{coreg} corresponds to the worst-case scenario leading to the largest cost value among all possible sampling rate trajectories.

The optimization problem for the co-regulated controller design can be formulated by combining the above two arguments together as:

$$\begin{aligned} & \min_{u_p[k]} \ J_{coreg} \\ & \text{Subject to: } \Delta V(x_p[k], x_c[k]) < 0. \end{aligned} \tag{9}$$

To build a numerically tractable optimization problem, we leverage results from [10] to construct a correct-by-construction stable controller for co-regulated systems.

Theorem 1: For the co-regulated system in (6), assume there exists a set of control gain matrices $K_p(x_c)$ for each possible sampling rate value $x_c \in \Sigma$, and the control law

$$u_p[k] = -K_p(x_c[k]) x_p[k] \tag{10}$$

is applied at each time index k. The closed-loop co-regulated system is asymptotically stable for all sampling rate switching trajectories if there exists $P = P^T > 0$ such that

$$\begin{aligned} & \mathcal{A}(x_c)^T P \mathcal{A}(x_c) - P + Q_1(x_c) - Q_{12}(x_c) K_p(x_c) - \\ & K_p(x_c)^T Q_{12}(x_c)^T + K_p(x_c)^T Q_2(x_c) K_p(x_c) < 0 \end{aligned} \tag{11}$$

can be met for all $x_c \in \Sigma$. $\mathcal{A}(x_c)$ is defined in (6), $Q_1(x_c)$, $Q_2(x_c)$ and $Q_{12}(x_c)$ are calculated based on (8) for all possible sampling rate values in Σ. Moreover, the upper bound of the infinite horizon cost in (9) can be denoted as

$$J_{coreg} = x_p[0]^T P x_p[0], \tag{12}$$

where $x_p[0]$ is the initial state.

Proof: The uncertainty of the sampling rate $x_c[k]$ trajectory brings challenges in constructing a time-varying Lyapunov function parameter $P(x_c[k])$. Since our goal is to synthesize stable controllers, we can choose $P(x_c[k]) = P > 0$ to construct a common Lyapunov function $V(x_p[k], x_c[k]) = x_p[k]^T P x_p[k]$ $\forall x_c \in \Sigma$. V satisfies $\alpha_2(\|x_p[k]\|) = \lambda_{\max}(P) \|x_p[k]\|^2$ where $\lambda_{\max}$ is the largest eigenvalue, and $\alpha_1(\|x_p[k]\|) = \sigma \|x_p[k]\|^2$ where σ is a small positive scalar. The difference of the Lyapunov function along the solution of (6) is given by

$$\begin{aligned} & \Delta V(x_p[k], x_c[k]) = V(x_p[k+1], x_c[k+1]) - \\ & V(x_p[k], x_c[k]) = x_p[k]^T (\mathcal{A}(x_c[k])^T P \mathcal{A}(x_c[k]) - P) x_p[k]. \end{aligned}$$

Further, based on the constraints in (11), we conclude:

$$\begin{aligned} & \Delta V(x_p[k], x_c[k]) < -x_p[k]^T (Q_1[k] - Q_{12}[k] K_p(x_c[k]) - \\ & K_p(x_c[k])^T Q_{12}[k]^T + K_p(x_c[k])^T Q_2[k] K_p(x_c[k])) x_p[k]. \end{aligned} \tag{13}$$

Substituting $Q_1[k]$, $Q_{12}[k]$ and $Q_2[k]$ from (8) into (13), the right hand side becomes

$$\begin{aligned} & -x_p[k]^T \int_0^{\frac{1}{x_c[k]}} (\Phi(\tau) - \Gamma(\tau) K_p(x_c[k]))^T Q (\Phi(\tau) - \Gamma(\tau) K_p(x_c[k])) d\tau \ x_p[k] \\ & -x_p[k]^T \int_0^{\frac{1}{x_c[k]}} (\Gamma(\tau) K_p(x_c[k]))^T R (\Gamma(\tau) K_p(x_c[k])) d\tau \ x_p[k]. \end{aligned}$$

This implies $\Delta V(x_p[k], x_c[k]) < 0$ for all non-zero states [10], hence the co-regulated system is asymptotically stable for all possible sampling rate trajectories.

Then, we need to prove the upper bound of the infinite horizon cost is (12). Since the resulting closed-loop system is asymptotically stable, then $x_p[\infty] = 0$ and $V(x_p[\infty], x_c[\infty]) = 0$. By summing (13) from $k = 0$ to ∞, based on the control law defined in (10), we get $x_p[0]^T P x_p[0] > \sum_{k=0}^{\infty} J[k]$, where $J[k]$ is defined in (7) as the cost at time index k. Thus J_{coreg} can be selected as $x_p[0]^T P x_p[0]$. ■

With this result the controller design can be recast as follows: synthesize a set of constant feedback gain matrices, $K_p(x_c)$, $\forall x_c \in \Sigma$, such that the control law (10) can minimize the cost function (12) while satisfying the stability constraints in (11). Solving the corresponding Riccati inequalities in (11) will provide P, and hence the controller gain matrices, $K_p(x_c)$, for a co-regulated system. However, a solution can not be obtained conveniently since (11) is not convex [10].

From [10], we leverage an efficient method to solve this problem by formulating the stability constraints in (11) as a set of Linear Matrix Inequalities (LMI) $\forall x_c \in \Sigma$,

$$\begin{bmatrix} W_0 & (\Phi(x_c) W_0 - \Gamma(x_c) W(x_c))^T & \begin{bmatrix} W_0 & -W(x_c)^T \end{bmatrix} \\ \Phi(x_c) W_0 - \Gamma(x_c) W(x_c) & W_0 & 0 \\ \begin{bmatrix} W_0 \\ -W(x_c) \end{bmatrix} & 0 & Q(x_c)^{-1} \end{bmatrix} > 0. \tag{14}$$

where $W_0 = P^{-1}$, $W(x_c) = K_p(x_c)P^{-1}$, I is the identity matrix and

$$Q(x_c) = \begin{bmatrix} Q_1(x_c) & Q_{12}(x_c) \\ Q_{12}(x_c)^T & Q_2(x_c) \end{bmatrix}. \tag{15}$$

The satisfaction of all LMIs in (14) provides stability constraints for the optimization. The objective function for the optimization is $J_{coreg} = x_p[0]^T P x_p[0]$. It is equivalent to minimize the trace of P or W_0^{-1} [10], although the problem is now non-convex. A convex equivalent can be had by minimizing $\log(\det(W_0^{-1}))$ [10]. Thus the controller synthesis algorithm for co-regulated system can be summarized as:

$$\begin{aligned} &\min_{W_0, W(x_c)} \log(\det(W_0^{-1})) \\ &\text{subject to: } W_0 = W_0^T > 0, \text{ validate (14) } \forall x_c \in \Sigma. \end{aligned} \tag{16}$$

Then the set of control matrices $K(x_c)$ can be achieved as:

$$K(x_c) = W(x_c)W_0^{-1}, \quad \forall x_c \in \Sigma. \tag{17}$$

This control strategy provides an explicit solution for co-regulated systems by calculating control gain matrices corresponding to each sampling rate. The asymptotic stability of the co-regulated system can be guaranteed for all possible sampling rate trajectories. This analysis is focused on a discrete-time co-regulated system model (6) that captures the behavior of the continuous model (1) at sampling times. The results from related literature (Proposition 16 in [4]) has shown that for a Linear Time-Invariant (LTI) sampled data system, the asymptotic stability in continuous-time and in discrete-time are equivalent. Thus the asymptotic stability of the continuous-time co-regulated system model (1) can also be guaranteed.

IV. Online Solution - MPC for Co-regulation

The explicit control strategy in Section III provides a stable but conservative solution since the optimization problem is constructed as minimizing the upper bound of the infinite horizon cost among all possible sampling rate trajectories. However, the sampling rate trajectory of a co-regulated system is propagated based on the computational system control model in (4) and (5). This allows us to design a co-regulated MPC strategy that predicts both system states and sampling rate trajectories within the prediction horizon based on the current measurements. The proposed control algorithm builds on hybrid MPC design for Linear Parameter Varying (LPV) systems [11], with the unique feature of predicting both system states and sampling rate trajectories within the receding horizon.

The goal is to provide an optimal feedback control law

$$u_p[k] = u^*(x_p[k], x_c[k]) \tag{18}$$

depending on the current state value, $x_p[k]$, and sampling rate value, $x_c[k]$. Following the receding horizon control strategy, only the first computed control input in the solution sequence, u^*, is applied to the plant during the current time index, k. At the next time index, a new MPC problem based on new measurements is solved over a shifted horizon. We define the cost function for co-regulated systems as

$$\begin{aligned} J(x_p[k], u_p[k]) &= x_p[k+N]^T P x_p[k+N] + \\ &\sum_{i=0}^{N-1} \left(x_p[k+i]^T Q x_p[k+i] + u_p[k+i]^T R u_p[k+i] \right), \end{aligned} \tag{19}$$

where P, Q, R are symmetric positive definite matrices.

The co-regulated MPC problem is then constructed as

$$u_p[k] = u^*(x_p[k], x_c[k]) = \arg\min_{u_p} J(x_p[k], u_p[k])$$

Subject to:

$$\begin{aligned} &x_p[k+i+1] = \Phi(x_c[k])x_p[k+i] + \Gamma(x_c[k])u_p[k+i], \\ &u_c[k+i] = K_{cp} \left\| x_p[k+i] \right\| - K_c \left(x_c[k+i] - x_{c,ref} \right), \\ &x_c'[k+i+1] = x_c[k+i] + \frac{1}{x_c[k+i]} u_c[k+i], \\ &x_c[k+i+1] = x_c'[k+i+1] \text{ rounded to nearest value in } \Sigma, \\ &x_p[k+i+1] \in \mathbb{X}, \ x_p[k+N] \in \mathbb{X}_f, \ u_p[k+i] \in \mathbb{U}, \end{aligned} \tag{20}$$

where $\mathbb{X}$, $\mathbb{U}$, and $\mathbb{X}_f$ are state, control, and terminal state constraints and are convex polytopes. The closed-loop stability and feasibility of the co-regulated system under MPC can be ensured by choosing the appropriate terminal weight, P, and terminal set, $\mathbb{X}_f$, leveraging the results from [12]–[14].

It has been shown that for LPV systems, if the terminal set $\mathbb{X}_f$ is configured as the maximal positive invariant set [15] for the closed-loop system for all affecting parameters, the receding horizon control problem is persistently feasible [14]. For co-regulated systems (6), the terminal set can be configured as $\mathcal{O}_\infty^{LQR}$. $\mathcal{O}_\infty^{LQR}$ is associated with the state and input constraints and defined as the maximum positive invariant set for all $x_c \in \Sigma$ of the multi-model closed-loop system $x_p[k+1] = \mathcal{A}(x_c)x_p[k]$, where $\mathcal{A}(x_c) = \Phi(x_c) - \Gamma(x_c)K_{LQR}(x_c)$, $K_{LQR}(x_c)$ denotes the LQR gains associated with sampling rate x_c. The co-regulated MPC problem (20) is feasible for all $k \geq 0$ if $\mathbb{X}_f = \mathcal{O}_\infty^{LQR}$ and if $x_p[0] \in \kappa_N(\mathcal{O}_\infty^{LQR})$. κ_N denotes the N-step controllable set, indicating there exists a sequence of N inputs that evolves the system to the set $\mathcal{O}_\infty^{LQR}$ while satisfying the constraints. The proof for feasibility of this LPV-MPC problem can be found in [14]. We leverage the method in [14] to calculate the $\mathcal{O}_\infty^{LQR}$ for our co-regulated UAS model. The maximum positive invariant sets for the discrete UAS models corresponding to each possible sampling rate values $x_c \in \Sigma$ are computed considering the state and control constraints, then $\mathcal{O}_\infty^{LQR}$ can be achieved as the invariant set for all $x_c \in \Sigma$ [14]. The operations calculating $\mathcal{O}_\infty^{LQR}$ can be performed using the Multi-Parametric Toolbox (MPT) in MATLAB [16].

To guarantee the co-regulated MPC stability, we extend the method in [13] to construct the terminal weight matrix P to determine the terminal cost. The conventional approach to guarantee stability for LTI system with an MPC controller is to select P as the solution of the algebraic Riccati equation [13]. A co-regulated system contains a set of solutions for the Riccati equations corresponding to each $x_c \in \Sigma$ (e.g., $P(x_c)$). An upper bound of the terminal cost needs to be determined among all models in the multi-model description. The P value in co-regulated MPC (19) must be satisfied $\forall x_c \in \Sigma$ [13]

$$\mathcal{A}(x_c)^T P \mathcal{A}(x_c) + K_{LQR}(x_c)^T R K_{LQR}(x_c) + Q - P \leq 0, \tag{21}$$

Different ways to find P are introduced in [13], [14], but P must satisfy all LMIs in (21) to guarantee stability.

Theorem 2: Consider the co-regulated system model (2) and optimal control law (19), (20). Assume $\mathbb{X}$, $\mathbb{X}_f$, $\mathbb{U}$ are closed and contain the origin in their interior, and $\mathbb{X}_f$ is control invariant

This article has been accepted for publication in a future issue of this journal, but has not been fully edited. Content may change prior to final publication. Citation information: DOI 10.1109/LCSYS.2020.3044261, IEEE Control Systems Letters

and $\mathbb{X}_f \subseteq \mathbb{X}$ [14]. If the terminal weight, P, satisfies inequality constraints (21), and the terminal constraint $\mathbb{X}_f$ is chosen as $\mathcal{O}_\infty^{LQR}$, the origin of the closed-loop co-regulated system is asymptotically stable with domain of attraction $\kappa_N(\mathcal{O}_\infty^{LQR})$.

Proof: Consider the co-regulated MPC problem (20) at time index k. Let $x_p[k] \in \kappa_N(\mathcal{O}_\infty^{LQR})$ and let $U^* = \{u_p[k]^*, u_p[k+1]^*, \ldots, u_p[k+N-1]^*\}$ be the optimizer of problem (20) and $X_p^* = \{x_p[k], x_p[k+1]^*, \ldots, x_p[k+N]^*\}$ be the corresponding optimal state trajectory. After implementing the optimal control input $u_p[k]^*$, the next state $x_p[k+1]$ is achieved. Let $J^*(x_p[k])$ be the optimal total predicted cost of (20) when applying the control U^* to the system state $x_p[k]$. Considering the co-regulated MPC problem (20) at time index $k+1$, we attempt to construct an upper bound on $J^*(x_p[k+1])$.

Consider the sequence $\tilde{U}_1 = \{u_p[k+1]^*, \ldots, u_p[k+N-1]^*, -K_{LQR}(x_c[k+N])x_p[k+N]\}$. Then the corresponding state trajectory with this control sequence is $\tilde{X}_1 = \{x_p[k+1]^*, \ldots, x_p[k+N]^*, \mathcal{A}(x_c[k+N])x_p[k+N]^*\}$. Because $\tilde{U}_1$ is not the optimum for (20), $J(x_p[k+1], \tilde{U}_1)$ is an upper bound of $J^*(x_p[k+1])$. Then

$$\begin{aligned} &J(x_p[k+1], \tilde{U}_1) - J^*(x_p[k]) = -(x_p[k]^T Q x_p[k] + u_p[k]^{*T} R u_p[k]^*) \\ &+ x_p[k+N]^{*T}(\mathcal{A}(x_c[k+N])^T P \mathcal{A}(x_c[k+N]) + Q \\ &+ K_{LQR}(x_c[k+N])^T R K_{LQR}(x_c[k+N]) - P) x_p[k+N]^*. \end{aligned} \tag{22}$$

Since the condition in (21) can be met for all possible values of $x_c \in \Sigma$, and Q, R are positive definite, the right-hand side of (22) is negative definite. Moreover, since by construction $J^*(x_p[k+1]) \leq J(x_p[k+1], \tilde{U}_1)$, we can further infer $J^*(x_p[k+1]) - J^*(x_p[k]) < 0$ for all non-zero states, x_p.

To prove stability, we need to establish that $J^*(x_p)$ is a Lyapunov function. $J^*(x_p)$ is positive definite due to the symmetric positive definite P, Q, and R matrices. $J^*(x_p)$ decreases along the closed-loop trajectories as discussed above. It has been shown in [12] (Theorem 12.2) that $J^*(x_p)$ is continuous and $J^*(x_p) \leq x_p^T P x_p$ based on the assumptions in the theorem and constraints (21). Thus $J^*(x_p)$ is a Lyapunov function, and the origin of the closed loop co-regulated system is asymptotically stable if the initial state lies in $\kappa_N(\mathcal{O}_\infty^{LQR})$. ■

V. Results - Co-regulated UAS

We apply the proposed explicit IHC and MPC strategies to a co-regulated quadcopter UAS to verify the design effectiveness. The UAS state consists of the vehicle's position $(x, y, z)^T$, velocity in $\mathbb{R}^3$, orientation in roll (ϕ), pitch (θ), and yaw (ψ) angles, and angular rate of change in yaw

$$x_p = \left(x, y, z, \phi, \theta, \psi, \dot{x}, \dot{y}, \dot{z}, \dot{\psi}\right)^T.$$

The UAS comes equipped with an embedded inner-loop attitude feedback controller which accepts as inputs the desired thrust, T, roll angle, ϕ, pitch angle, θ and body yaw rate, r. Thus the control input, $u_p = (\phi, \theta, r, T)^T$. The equations governing the translational motions are

$$\begin{bmatrix} \ddot{p}_n \\ \ddot{p}_e \\ \ddot{p}_d \end{bmatrix} = -\frac{T}{m} \begin{bmatrix} \cos\phi \sin\theta \cos\psi + \sin\phi \sin\psi \\ \cos\phi \sin\theta \sin\psi - \sin\phi \cos\psi \\ \cos\phi \cos\theta \end{bmatrix} + \begin{bmatrix} 0 \\ 0 \\ g \end{bmatrix}$$

where m is the total mass of the UAS, and g is gravity. We leverage these nonlinear equations for high-fidelity simulation, and use a linearized state-space system model about a stable hover for control design leading to a linear state-space model like (1).

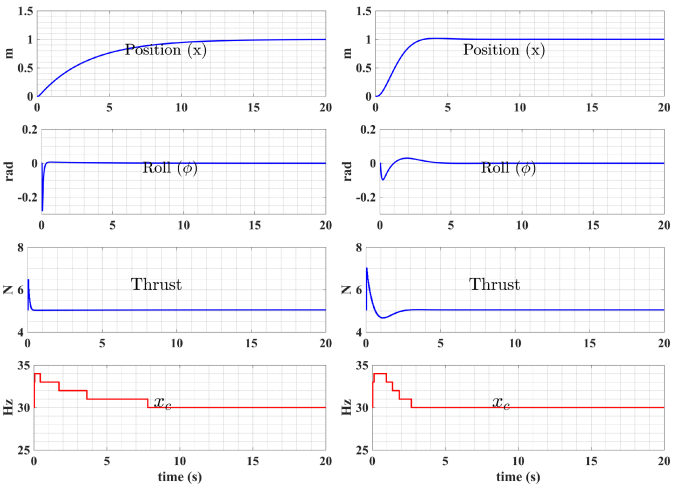

(a) Explicit IHC (b) Co-regulated MPC

Fig. 2: Step response of explicit IHC and Co-regulated MPC.

The sampling rate trajectory of the co-regulated UAS is regulated by the computational system model (5) and controller controller (4). For the physical system control design, we use the same manually tuned Q and R parameters for both explicit IHC and co-regulated MPC design. The prediction horizon length of the MPC is manually tuned as $N = 4$ to achieve a sufficient control performance while obtain fast solutions for the MPC problem. Variations in the system state, inputs, and sampling rate are shown for a step response in Figure 2 for each control strategy.

The step responses in Figure 2 show that the system under explicit IHC controller evolves much slower than the co-regulated MPC controller and the settling time of the explicit IHC controller is approximately four times longer than the MPC controller. Because explicit IHC minimizes the upper bound of the "worst-case" infinite horizon cost value among all possible sampling rate trajectories without considering the computational system model, it is a much more conservative approach than co-regulated MPC. Co-regulated MPC constructs a finite horizon cost function for the optimization problem at each sampling instance based on the predicted sampling rate trajectory according to the computational system model and the current state measurement. The gains of the explicit IHC are much less aggressive than the co-regulated MPC strategy. As a result, this incurs a smaller overshoot (appoximately 0.1%) in position. The slower converging speed of explicit IHC leads to a higher usage of computational resources. The computational controller will reallocate more resources to the control task in response to the higher physical state error during the converging process. However, explicit IHC requires much less computational to provide the control input since control gains are pre-computed offline and can be implemented as a look-up table for online execution. In our tests, while explicit IHC requires a computation time of less than 0.4 ms for each

step, co-regulated MPC requires 0.1 - 0.2 s since it requires solving a mixed-integer quadratic programming problem at each step. The computations for this work were performed on a 2.3 GHz Intel i5 processor using MATLAB R2017a. The co-regulated MPC problem was solved by leveraging the YALMIP toolbox [17] with Gurobi optimization solver [18]. Future work, such as extending the explicit MPC approach in [19], may reduce the online computation required for co-regulated MPC to be deployed onboard a small, computationally constrainted UAS.

Figure 3 shows the UAS executing a commanded trajectory under co-regulated MPC and explicit IHC controllers. As observed, the UAS evolves slowly to the reference waypoint with nearly no overshoot when controlled by the explicit IHC. In constrast, it evolves much faster with a relatively larger overshoot when controlled by MPC. Both explicit IHC and MPC can stabilize the co-regulated system under a time-varying sampling rate. In the test, we observed that the overshoot of the MPC controlled UAS can be decreased by increasing the prediction horizon length at the expense of more computation.

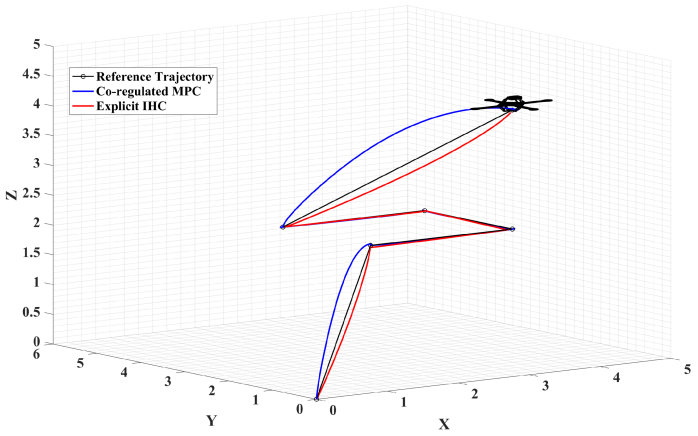

Fig. 3: Trajectory following performance for explicit IHC and co-regulated MPC

These results lead to an intuition for deploying different controllers for different working scenarios. For a co-regulated system with slow dynamics, the explicit IHC controller can provide smooth, stable control. For systems requiring faster responses, the co-regulated MPC controller is capable of providing more aggressive maneuvers but requires more online computation time.

VI. Conclusion

In this paper we presented two stability guaranteed controllers for a class of time-varying periodic sampling, co-regulated systems. We first provided an explicit infinite horizon control (IHC) design by drawing from specialized results for an LPV system. A correct-by-construction stability constraint was customized for co-regulated system structures when constructing the offline optimization problem. The resulting gain matrices for each possible co-regulated system sampling rate value can found to guarantee stability for arbitrary sampling rate switchings. However, unlike conventional LPV systems, co-regulated systems are capable of predicting the future sampling rate trajectory based on the computational system model. To leverage this we proposed a MPC strategy for co-regulated systems where both the system state trajectory and the sampling rate trajectory are predicted within the receding horizon. The feasibility and stability of the co-regulated MPC was presented. Simulation results for a co-regulated multicopter UAS were presented to demonstrate the effectiveness and tradeoffs of the two control strategies.

References

[1] W. Heemels, M. C. F. Donkers, and A. R. Teel, "Periodic event-triggered control for linear systems," *IEEE Transactions on Automatic Control*, vol. 58, no. 4, pp. 847–861, 2013.

[2] W. Heemels, K. H. Johansson, and P. Tabuada, "An introduction to event-triggered and self-triggered control," in *Decision and Control (CDC), 2012 IEEE 51st Annual Conference on*. IEEE, 2012, p. 3270–3285.

[3] J. M. Bradley and E. M. Atkins, "Coupled cyber-physical system modeling and coregulation of a cubesat," *IEEE Transactions on Robotics*, vol. 31, no. 2, p. 443–456, Apr. 2015.

[4] L. Hetel, C. Fiter, H. Omran, A. Seuret, E. Fridman, J.-P. Richard, and S. I. Niculescu, "Recent developments on the stability of systems with aperiodic sampling: An overview," *Automatica*, vol. 76, pp. 309–335, 2017.

[5] X. Zhang, S. Doebbeling, and J. Bradley, "Co-regulation of computational and physical effectors in a quadrotor unmanned aircraft system," in *Proceedings of the 9th ACM/IEEE International Conference on Cyber-Physical Systems*. IEEE Press, 2018, pp. 119–129.

[6] X. Zhang and J. Bradley, "Stability analysis for a class of resource-aware, co-regulated systems," in *2019 IEEE 58th Conference on Decision and Control (CDC)*. IEEE, 2019, pp. 193–200.

[7] K. J. Åström and B. Wittenmark, *Computer-controlled systems: theory and design*. Courier Corporation, 2013.

[8] H. Lin and P. J. Antsaklis, "Stability and stabilizability of switched linear systems: a survey of recent results," *IEEE Transactions on Automatic control*, vol. 54, no. 2, pp. 308–322, 2009.

[9] J. Daafouz and J. Bernussou, "Parameter dependent lyapunov functions for discrete time systems with time varying parametric uncertainties," *Systems & control letters*, vol. 43, no. 5, pp. 355–359, 2001.

[10] M. Schinkel and W.-H. Chen, "Control of sampled-data systems with variable sampling rate," *International journal of systems science*, vol. 37, no. 9, pp. 609–618, 2006.

[11] M. M. Morato, J. E. Normey-Rico, and O. Sename, "Model predictive control design for linear parameter varying systems: A survey," *Annual Reviews in Control*, 2020.

[12] F. Borrelli, A. Bemporad, and M. Morari, *Predictive control for linear and hybrid systems*. Cambridge University Press, 2017.

[13] P. F. Lima, J. Mårtensson, and B. Wahlberg, "Stability conditions for linear time-varying model predictive control in autonomous driving," in *2017 IEEE 56th Annual Conference on Decision and Control (CDC)*. IEEE, 2017, pp. 2775–2782.

[14] P. F. Lima, G. C. Pereira, J. Mårtensson, and B. Wahlberg, "Experimental validation of model predictive control stability for autonomous driving," *Control Engineering Practice*, vol. 81, pp. 244–255, 2018.

[15] E. G. Gilbert and K. T. Tan, "Linear systems with state and control constraints: The theory and application of maximal output admissible sets," *IEEE Transactions on Automatic control*, vol. 36, no. 9, pp. 1008–1020, 1991.

[16] M. Herceg, M. Kvasnica, C. N. Jones, and M. Morari, "Multi-parametric toolbox 3.0," in *2013 European control conference (ECC)*. IEEE, 2013, pp. 502–510.

[17] J. Lofberg, "Yalmip: A toolbox for modeling and optimization in matlab," in *2004 IEEE international conference on robotics and automation (IEEE Cat. No. 04CH37508)*. IEEE, 2004, pp. 284–289.

[18] G. OPTIMIZATION, "Inc. gurobi optimizer reference manual, 2015," *URL: http://www. gurobi. com*, p. 29, 2014.

[19] T. Besselmann, J. Lofberg, and M. Morari, "Explicit mpc for lpv systems: Stability and optimality," *IEEE Transactions on Automatic Control*, vol. 57, no. 9, pp. 2322–2332, 2012.